Geophysical Research Letters

RESEARCH LETTER
10.1029/2023GL106735

Direct Observation of the Space Hurricane Disturbed Polar Thermosphere

Zhi-Feng Xiu[1], Yu-Zhang Ma[1], Qing-He Zhang[1], Zan-Yang Xing[1], Shun-Rong Zhang[2], Yong-Liang Zhang[3], Kjellmar Oksavik[4,5], Larry Lyons[6], Michael Lockwood[7], and Yong Wang[1]

[1]Shandong Provincial Key Laboratory of Optical Astronomy and Solar-Terrestrial Environment, Institute of Space Sciences, Shandong University, Weihai, China, [2]MIT Haystack Observatory, Westford, MA, USA, [3]The Johns Hopkins University Applied Physics Laboratory, Laurel, MD, USA, [4]Department of Physics and Technology, University of Bergen, Bergen, Norway, [5]Arctic Geophysics, University Centre in Svalbard, Longyearbyen, Norway, [6]Department of Atmospheric and Oceanic Sciences, University of California, Los Angeles, CA, USA, [7]Department of Meteorology, University of Reading, Reading, UK

Key Points:

- The space hurricane can relocate the reversal of the neutral wind from the auroral oval to the edge of the space hurricane
- The space hurricane can heat the thermosphere and generate Atmospheric gravity waves (AGWs) that disturb the neutral density and vertical wind
- The space hurricane can significantly enhance polar cap AGW activity in the dawn sector

Supporting Information:

Supporting Information may be found in the online version of this article.

Correspondence to:

Y.-Z. Ma,
myz0103@sina.com

Citation:

Xiu, Z.-F., Ma, Y.-Z., Zhang, Q.-H., Xing, Z.-Y., Zhang, S.-R., Zhang, Y.-L., et al. (2024). Direct observation of the space hurricane disturbed polar thermosphere. *Geophysical Research Letters*, *51*, e2023GL106735. https://doi.org/10.1029/2023GL106735

Received 13 OCT 2023
Accepted 18 DEC 2023

Abstract The space hurricane is a three-dimensional magnetic vortex structure with strong flow shears and electron precipitation in the polar cap. This study investigates for the first time how a space hurricane disturbs the polar thermosphere. During the formation and development of the space hurricane, the directional reversal of the horizontal neutral wind and the plasma convection will both be relocated from the poleward auroral oval boundary to the edge of the space hurricane, but the neutral wind responds slower compared to the plasma convection. Strong flow shears in the space hurricane causes enhanced Joule heating in the polar cap, which heats the thermosphere and triggers Atmospheric Gravity Waves (AGWs). Statistical results reveal that significant AGWs mainly are located on the dawnside of the space hurricane, suggesting that the space hurricane plays a significant role in ion-neutral coupling and generation of polar cap AGWs.

Plain Language Summary The space hurricane is a cyclonic aurora structure over the Earth's polar cap region under northward interplanetary magnetic field condition. It can transfer large amounts of energy and plasma into the polar ionosphere during otherwise extremely quiet geomagnetic times. Joule/Frictional heating due to ion-neutral collisions plays a key role for the energy budget, resulting in non-negligible atmospheric disturbances, which may impact the orbits of low-altitude satellites through enhanced frictional drag. Using in situ observations from the Defense Meteorological Satellite Program satellites and the Gravity Field and Steady-State Ocean Circulation Explorer satellite, we report the first evidence of a disturbed thermosphere triggered by a space hurricane. The neutral wind shows a slow variation in response to the space hurricane plasma convection. Significant wave-like thermospheric density and vertical wind disturbances are observed around the space hurricane. Enhanced Joule heating from flow shears inside the space hurricane may be the generator. These findings show that the space hurricane plays a significant role for ion-neutral coupling in the polar cap region.

1. Introduction

The ion-neutral interaction plays a crucial role in ionosphere-thermosphere coupling. During periods of enhanced geomagnetic activity such as geomagnetic storm and substorm, energy is deposited into the auroral zones via particle precipitation and enhanced convection. These heat the local ionospheric plasma and couple via collisions to the neutral constituents of the thermosphere.

In the polar region, the neutral wind typically exhibits a circulation pattern that to the first order looks like the ionospheric convection. On the dawnside the neutral wind is significantly reduced due to the balance between the roughly anti-sunward pressure gradient, the ion drag, and the Coriolis force. In the duskside auroral oval the higher ion density and ion drag driven by electric fields work together with the Coriolis force to overcome the opposing pressure gradient, which leads to a strong sunward neutral wind (Kiene et al., 2018). Frictional heating caused by collisions between ions and neutrals, also known as Joule heating, plays an important role in the energy budget of the upper polar thermosphere (Fujii et al., 1998; Sojka, 2017; Stubbe & Chandra, 1971). Modeling work shows that after a sudden enhancement of the ion convection, Joule heating increases at all altitudes due to the enhancement of the difference between the ion convection and neutral wind velocity (Deng et al., 2011).

These heating processes can lead to the generation of Atmospheric Gravity Waves (AGWs) in the polar thermosphere (Hunsucker, 1982; Millward et al., 1993; Oyama et al., 2001; Shinagawa & Oyama, 2006), which may cause trans-polar traveling ionospheric disturbances (S.-R. Zhang et al., 2019). Large upward and downward winds appear in a region poleward of the poleward auroral oval boundary, extending over several degrees in latitude (Price et al., 1995), and several hours in local time (Innis et al., 1999).

Several studies have focused on the ion-neutral momentum coupling, primarily in the auroral oval region. However, the effects of polar cap aurora on the thermosphere are not well understood and require further investigation. The space hurricane has been reported as a large-scale three-dimensional magnetic vortex structure in the polar cap (Q.-H. Zhang et al., 2021). The space hurricane has strong circular horizontal plasma flow shears, and a cyclone-shaped aurora accompanied by strong electron precipitation and intense upward field-aligned currents. However, it has not yet been determined whether the modified convection pattern and particle deposition in the polar cap can influence the upper thermosphere. In this work, we present a direct observation of the space hurricane disturbed thermosphere on 15 June 2010 and a statistical study from January 2010 to October 2013.

2. Data and Methods

2.1. GOCE Data

Gravity Field and Steady-State Ocean Circulation Explorer (GOCE) is a thermospheric satellite in a near-circular dusk–dawn orbit at an inclination of 96.7°, with an orbital period of ∼101 min. It has a time resolution of 10 s and an average speed of ∼8 km/s (Quang et al., 2018). Six Onboard-accelerometers allow for the observation of cross-track neutral wind data which includes zonal, meridional and vertical components, and neutral density. Consequently, in the polar region, measured neutral wind is mainly sunward-antisunward.

To investigate the influence of space hurricanes on neutral winds, the fluctuation of vertical wind and neutral density is calculated using a 12-points Savitzky-Golay filter to investigate the potential AGWs (S.-R. Zhang et al., 2017, 2019). The algorithm uses a convolution process with least squares fitting of successive subsets of windows of a given length.

2.2. DMSP Data

The Defense Meteorological Satellite Program (DMSP) satellites are in a polar dusk-dawn orbit at an altitude of ∼860 km, with an orbital period of ∼110 min. For this study, we utilized (a) the ion velocity, density, and temperature at a time resolution of 4 s, (b) the energy flux of ions and electron precipitation at a time resolution of 1 s in the energy range of 30 eV to 30 keV (Hardy et al., 1984) and (c) the magnetic field fluctuation at a time resolution of 1 s (Rich & Hairston et al., 1994) from DMSP F16 observations. The Special Sensor Ultraviolet Spectrographic Imagers (SSUSI) carried by DMSP provides cross-track scanned images of the 2-D aurora pattern. In this paper, N_2 Lyman-Birge-Hopfield short band (140.0–150.0 nm) is used for visualizing the structure of space hurricane.

3. Observation and Discussion

3.1. Ion Convection and Horizontal Neutral Wind

In this study, we focus on four DMSP F16 and GOCE polar tracks in the northern polar cap, which are indicated in Figures 1a and 1b by four red dash lines corresponding to Figures 1c–1f. Figures 1a and 1b provide an overview of a B_y dominated interplanetary magnetic field (IMF), under a quiet geomagnetic condition, with a substorm occurring. Detailed IMF, solar wind and geomagnetic indices are shown in Figure S1 in Supporting Information S1. Figures 1c–1f present the evolution of space hurricane, via a series of DMSP (black line) and GOCE (black dots, and colored dots indicating vertical wind speed) observation. The ion convection velocity from DMSP (horizontal cross-track ion velocity) and horizontal neutral wind from GOCE (horizontal cross-track neutral wind) are also plotted in magenta and green, respectively. The magenta and green stars represent the reversal position of ion convection velocity and horizontal neutral wind. The observation times of DMSP and GOCE are shown in magenta and green text, respectively. The DMSP and GOCE orbits are nearly parallel in the dusk sector, with time differences of just a few minutes to less than 30 min.

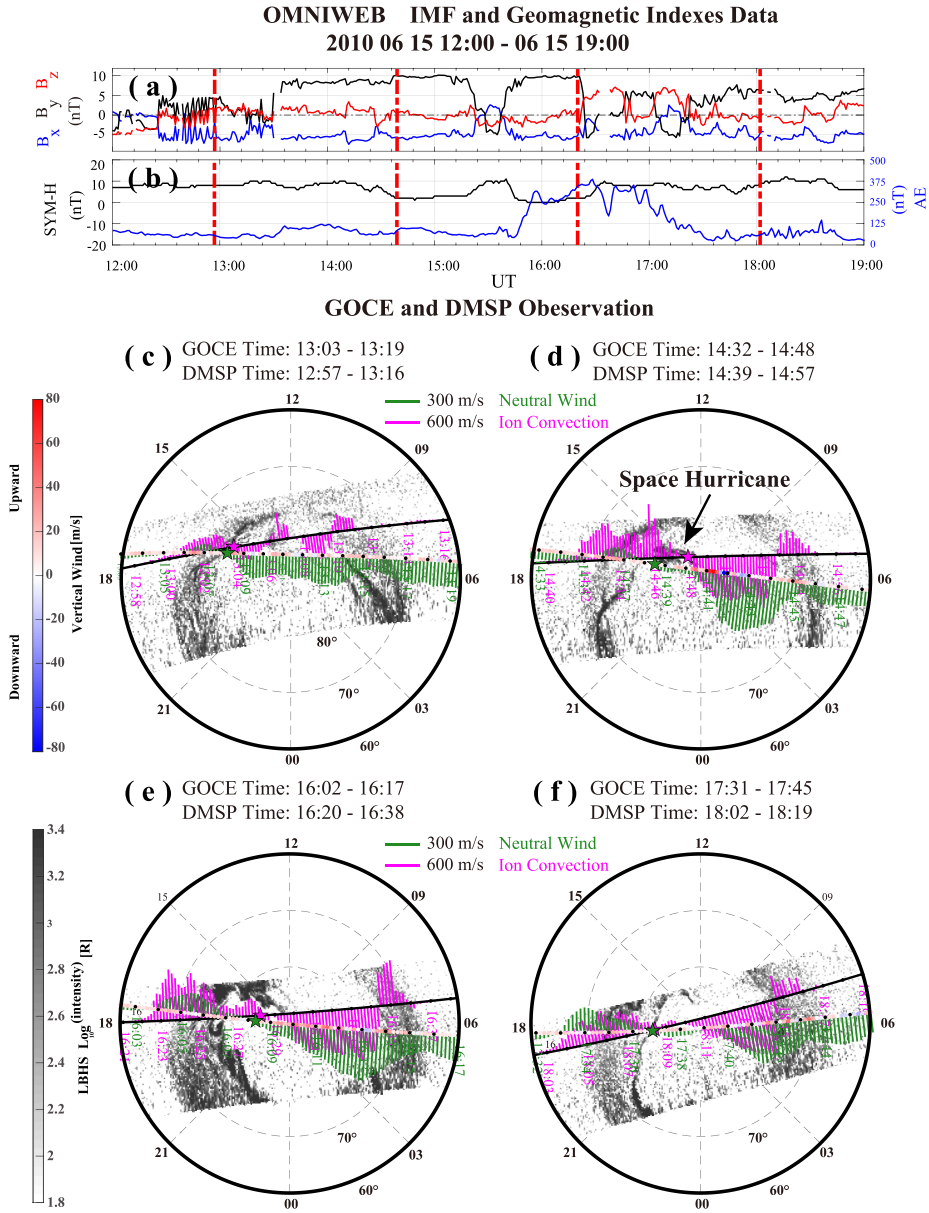

Figure 1. (a–b) Overview of interplanetary magnetic field and geomagnetic conditions during 12:00–19:00 UT on 15 June 2010. (c–f) A series of Defense Meteorological Satellite Program (DMSP) (black line) and Gravity Field and Steady-State Ocean Circulation Explorer (GOCE) (dots colored by red, white and blue) transits of the polar region. The ion convection velocity and horizontal neutral wind is also plotted in magenta and green colors, perpendicular to the DMSP and GOCE tracks, respectively. The magenta and green stars represent the cross-track velocity reversal boundaries near the aurora. The colored GOCE track includes the vertical neutral wind, where upward/downward is positive/negative. The black arrow identifies the space hurricane.

Figure 1c shows the appearance of a high latitude auroral spot under fluctuating, positive IMF B_z and dominant IMF B_y (Carter et al., 2020; Milan et al., 2000). The DMSP ion convection velocity reversed multiple times, suggesting convection vortices with reverse flows (Burch et al., 1980; Rich & Hairston, 1994; Vennerstrøm et al., 2002). The horizontal neutral wind was sunward in the duskside auroral oval and antisunward in the polar cap region. Both the neutral wind and the ion convection reversed at the poleward edge of duskside auroral oval.

After nearly two hours of stable and strongly positive B_y with northward IMF, a typical space hurricane with rotation-arms formed above 80° Magnetic Latitude in CGM coordinate (MLAT) and near 15 Magnetic Local Time in CGM coordinate (MLT) (Figure 1d, and clear SSUSI images are shown in Figure S7 in Supporting

Information S1). In the region of the space hurricane, the anti-sunward neutral wind was significantly weaker than before. Also, the reversal of both the ion convection and neutral wind migrated poleward from the auroral oval boundary (~78 MLAT) to the close vicinity of the space hurricane. However, the reversal of the neutral wind did not keep up with ions, as expected since the space hurricane modified the neutral wind through ion drag, but the neutral response was a slow process.

The IMF B_y component decreased at 15:20 UT and turned to negative until 15:50 UT and returned to 10 nT. During this period, DMSP F18 observed a fading of the space hurricane (Figure S2 in Supporting Information S1). As the Aurora Electrojet index (AE) index increased to 375 nT at 16:20 UT, Figure 1e shows that the auroral oval expanded poleward due to the associated substorm. A high-intensity auroral form lit up above 80° MLAT at 15 MLT and appeared to be related to the auroral oval. The ion drift remained sunward, which may be a result of both stable lobe B_y lobe reconnection in the northern hemisphere and expansion of the sunward convection in the auroral oval associated with the substorm. The neutral wind reversal moved further poleward to ~84 MLAT, almost identical to the reversal location of the ion drift.

About 1.5 hr later at 1802–1819 UT, the IMF turned to southward and the AE recovered to about 100 nT. Figure 1f shows that no discrete aurora observed in the polar cap region, Meanwhile the ion drift and the neutral wind in the polar cap both returned to anti-sunward. Thus, the flow reversals of both the ion drift and neutral wind migrated from about 84 MLAT back to the poleward edge of the auroral oval (~82 MLAT).

The horizontal neutral wind measured by GOCE and the ion velocity, electron and ion energy flux measured by DMSP are shown in Figure 2. The green/magenta dotted lines represent the reversal boundary of the horizontal neutral wind/ion convection velocity (V_y), respectively. The gray shaded region in Figure 2b illustrates the location of the space hurricane, which corresponds to the characteristic electron energy flux of 1 keV. Figure 2a includes that before the space hurricane appeared in the polar cap, the ion flow was sunward in the duskside auroral oval. As the satellite was moving dawnward, a cusp-ion-step like structure (Lockwood et al., 2001) associated with sunward ion flow was surrounded by anti-sunward ion flows, which may be caused by lobe reconnection under positive IMF Bz. The neutral wind was ~100 m/s sunward in the duskside auroral oval and was about 200–350 m/s antisunward throughout the dawnside. Both neutral wind and ion convection reversed at the poleward edge of the auroral oval at about 78° MLAT (Ma et al., 2018).

As seen in Figure 2b, within the space hurricane, located in the dusk side of the polar cap, the electron energy flux showed an inverted-V feature that was associated with the sunward-to-antisunward ion flow from the dusk side to the dawn side of the space hurricane (Q.-H. Zhang et al., 2021). The ion flow remained sunward in the dusk side auroral oval and the inverted-V feature, reversing to anti-sunward at 85.5° MLAT, 13:59 MLT and increasing to ~800 m/s as moving more dawnward. The neutral wind flow showed similar trend with the ion flow, with the wind being ~100 m/s sunward in the duskside auroral oval and strongly anti-sunward (~500 m/s) on the dawnside. The reversal boundary of neutral wind was shifted from 78° MLAT, 16:29 MLT to 81.5° MLAT, 16:46 MLT compared to Figure 2a. This indicates the ion flow changes caused by the space hurricane modified the neutral wind by ion drag, but the response of the dense neutrals was slower than for the ions due to their denser density and thermal pressure gradient dependence (Billett et al., 2020).

The time period of DMSP F18 observation in Figure S2 in Supporting Information S1 was between Figures 2b and 2c, which shows that ion drift remained sunward in the equatorward side of space hurricane. And later Figures 1e and 2c show that the enhanced duskside auroral oval was associated with strong sunward ion convection flow, likely due to the auroral substorm (AE = 375 nT) and strong positive IMF B_y during 15:50–16:20 UT. Due to the continuous ion drag, the sunward neutral wind region expanded poleward and the reversal latitude reached 84.1° MLAT, 17:42 MLT near the ion drift reversal (84.7° MLAT 17:08 MLT) in the polar cap region.

After 18:00 UT (Figure 2d), as the space hurricane faded and the substorm ended, the anti-sunward convection decreased and turned sunward inside the polar cap, and the neutral wind showed a similar trend. Thus, both the ion convection reversal and the neutral wind reversal moved back to the poleward edge of the auroral oval (82.0° MLAT 18:29 MLT, and 81.6° MLAT, 18:34 MLT, respectively). It is also worth noting that, the neutral wind velocity within the duskside polar cap, which was less than 100 m/s, remained much weaker than that in Figure 2a. This slow recovery indicates that the effects of space hurricane on the thermosphere linger for some time due to the long time constant for the neutrals to respond to a change in convection.

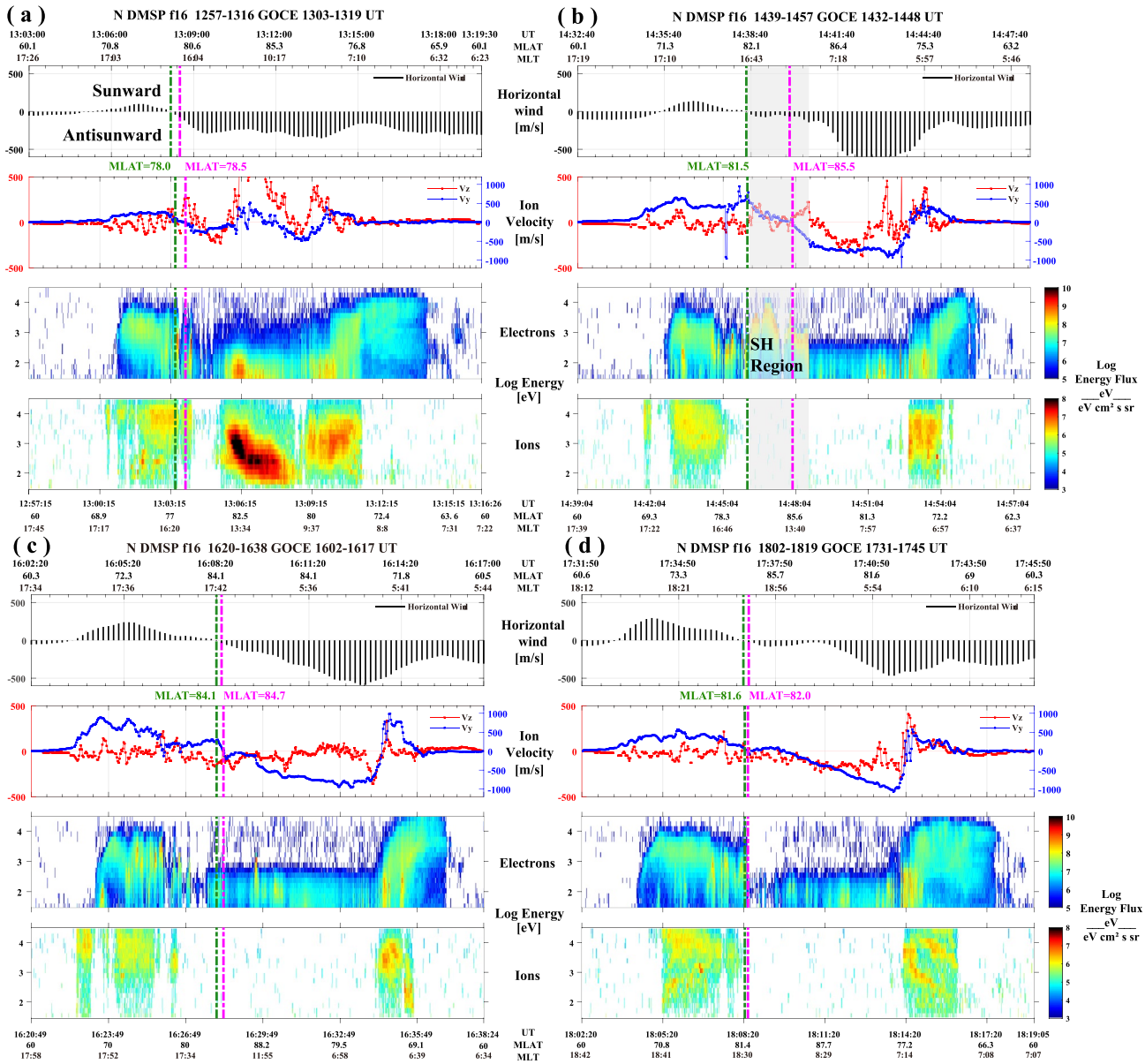

Figure 2. Each panel correspond to Figures 1c–1f. The Gravity Field and Steady-State Ocean Circulation Explorer (GOCE) orbit time and magnetic latitude is shown at the top. The Defense Meteorological Satellite Program (DMSP) orbit time, Magnetic Latitude in CGM coordinate and Magnetic Local Time in CGM coordinate is shown at the bottom. The green dotted lines represent the GOCE neutral wind reversal projected onto the DMSP measurements. The magenta dotted lines represent the DMSP V_y reversal projected onto the GOCE measurement. The space hurricane is shown as a gray shadow in panel (b). Each panel from top to bottom is: (1) GOCE horizontal wind, (2) DMSP cross-track and vertical ion velocity, (3) DMSP electron energy flux, (4) DMSP ion energy flux. The location of the ion and neutral wind reversals are indicated by magenta and green, respectively.

3.2. Atmospheric Gravity Waves

In Figure 1d, a fluctuation of vertical wind was also observed in the dawnside region of space hurricane as shown by on colored GOCE track. This fluctuation of vertical neutral wind in the polar region may be related to Atmosphere gravity waves (AGWs; Fedorenko, 2010). The raw data in Figure S3 in Supporting Information S1 shows that an obvious disturbance of neutral vertical wind and neutral density appeared on the dawn side of the space hurricane. To identify the AGWs from a slowly varying large-scale background, a 12 data points (corresponding to ~960 km along track) moving window low-pass Savitzky-Golay filter is applied on vertical wind and neutral density (Quang et al., 2018).

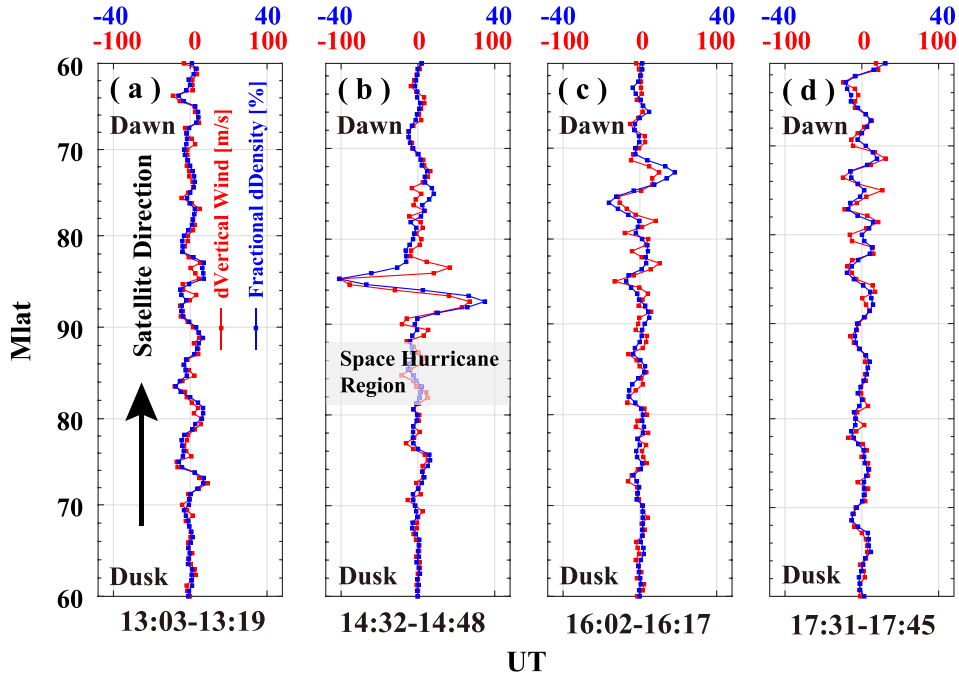

Figure 3. Each panel correspond to Figures 2a–2d. Gravity Field and Steady-State Ocean Circulation Explorer (GOCE) measured vertical wind (m/s) and fractional neutral density fluctuation (%) are plotted in red and blue, respectively. Bottom of every panel is the duskside, and the top is dawnside. GOCE satellite track direction is shown in panel (a) by black arrow, and is the same for other three panels. The space hurricane region is shown in shadow region in panel (b).

To identify the AGWs from a slowly varying large-scale background, a 12 data points (corresponding to ~960 km along track) moving window low-pass Savitzky-Golay filter is applied on vertical wind and neutral density to obtain the background signals (Quang et al., 2018). Then the filtering signals are obtained by subtracting the background signals from the original signals. The filtering result is shown in Figure 3: the detrended vertical wind (m/s) and fractional neutral density (%) fluctuation is plotted in red and blue, respectively.

The bottom of each panel is the duskside, and the top is dawnside. The GOCE satellite track direction is shown by a black arrow in Figure 3a. The space hurricane region is shown by the gray shaded region in Figure 3b by finding the closest position to both the dawn and dusk boundaries of the space hurricane along the GOCE orbit.

Figure 3a shows the polar region vertical wind and neutral density fluctuation in the polar cap region during quiet time (prior to the space hurricane). The vertical wind fluctuation was less than 20 m/s in magnitude, and the fractional neutral density fluctuation was around 5%. In Figure 3b, significant AGWs appeared in the dawnside of the space hurricane with a peak vertical wind fluctuation of 101 m/s and peak fractional change in neutral density of 41%, which were significant signals of AGWs (Innis & Conde, 2001, 2002). The observed wavelength of the space hurricane induced AGWs was about 600 km. However, the real wavelength was hard to estimate because the satellite may not travel in the same direction as the wavefront. Figure 3c shows that the fluctuation weakened (18% in density), and appeared at the auroral oval latitude, and this may be associated with the substorm (Innis & Conde, 2001, 2002). And it stayed there and seemed to influence more lower latitude as shown in Figure 3d.

Joule heating is a possible mechanism to generate AGWs (Hunsucker, 1982; Oyama & Watkins, 2012). Thus, we express the Joule heating rate as (Fujii et al., 1998; Thayer et al., 1995)

$$J \cdot E' = \sigma_p \left(E'\right)^2 \quad (1)$$

$$E' = (U - V) \times B \quad (2)$$

where σ_p is Pedersen conductivity, U is the neutral wind velocity, V is the ion velocity, and E' is the electric field in the reference frame of the neutral. Thus, Joule heating is clearly proportional to the square of the electric field E' in the neutral reference frame. In this study, the horizontal neutral wind U and ion velocity V were measured by GOCE and DMSP, and we also projected the DMSP ion velocity down to the GOCE altitude along magnetic field lines. Due to the nearly identical DMSP and GOCE orbit in both space and time, we conducted a qualitative analysis of the electric field along the satellite. The results shown in Figure S4 in Supporting Information S1 suggest there was an enhancement of Joule heating (indicated by E') accompanying AGWs in the vicinity of the space hurricane. This Joule heating caused by the strong flow shear between ions and neutrals may heat the thermosphere and further destroy the local thermosphere balance between gravity and buoyancy to generate AGWs (Deng et al., 2008, 2011; Guo et al., 2018).

3.3. Statistical Results

We also find a series of other AGWs events accompanying space hurricane using GOCE observations. Several identical cases (May-19, 2010; 16 June 2010; 15 July 2011 and 15 July 2013) are shown in S5. Furthermore, we conduct a statistics study in Northern Hemisphere from January 2010 to October 2013, to prove the AGWs around space hurricane is not occasional. Lu et al. (2022) provide the criteria to select space hurricanes from SSUSI data and a list of events. The space hurricane events during the statistics periods are selected from their list. Moving standard deviation of vertical wind $\sigma(W_z)$ is used to extract polar thermosphere AGWs activity (Innis & Conde, 2001; Visser et al., 2019). To calculate the $\sigma(W_z)$, we also conduct a 12 points moving window along the GOCE track. Considering the similar DMSP F16 and GOCE track in spatial and temporal scale, we identify the DMSP tracks which observed space hurricane, and then search for GOCE tracks having polar transit time no more than 30 min away from DMSP F16, to find the GOCE track with space hurricane. There are 1,367,946 data points along the selected spacecraft trajectories, 13,135 of these being associated with space hurricanes (146 space hurricane events). The SYM-H and AE mean values of those samples associated with space hurricane are about −5.2 and 151.6 nT, shown in Figure S6 in Supporting Information S1. This indicates that most space hurricanes occur during quiet magnetic periods.

Figure 4 shows MLT-MLAT maps of sample distribution and $\sigma(W_z)$, binned in 0.25 hr MLT and 2° MLAT. The sample distributions with and without space hurricane are roughly the same. The without space hurricane $\sigma(W_z)$ statistical result, Figure 4c, shows that AGWs are more active inside the polar cap than at lower latitudes, consistent with previous studies (Visser et al., 2019). The topology center positions of 146 space hurricane events are plotted in Figure 4d by black dots, which are mainly distributed within the noon and duskside polar cap. It is notable that when space hurricane happens, $\sigma(W_z)$ is significantly increased (maximizes 37 m/s) above 80 MLAT in the prenoon and noon sector, compared to that without space hurricane (maximizes 17 m/s). The AGWs activity enhanced region almost covers the space hurricane position (black dots in Figure 4d) and extends to the dawnside sector. This confirms that the AGWs may be caused by space hurricane and propagate to dawnside coinciding well with the event presented in details in this paper.

4. Conclusions

Using a combination of DMSP F16 and GOCE observations, we investigate the impact of the space hurricane disturbances on the polar upper thermosphere. For the first time, we identify such impact in the neutral wind. The space hurricane can weaken the intensity of and even reverse the direction of the horizontal neutral wind due to the continuous ion-neutral interaction via collisions in the polar cap. Significant AGWs are observed in the dawnside region of the space hurricane. The fluctuation of vertical wind can be up to 101 m/s in the region poleward of space hurricane, with an in-phase 41% neutral density fractional fluctuation. This indicates that space hurricane is an effective source of polar cap gravity waves and comparable with that of substorms (18% fractional density fluctuation observed). The statistics of 4-year GOCE neutral vertical wind observations also indicate that the appearance of the space hurricane will significantly enhance polar cap AGWs activity. Our results argue that the space hurricane can have important impact on the coupling of the ionosphere and the thermosphere.

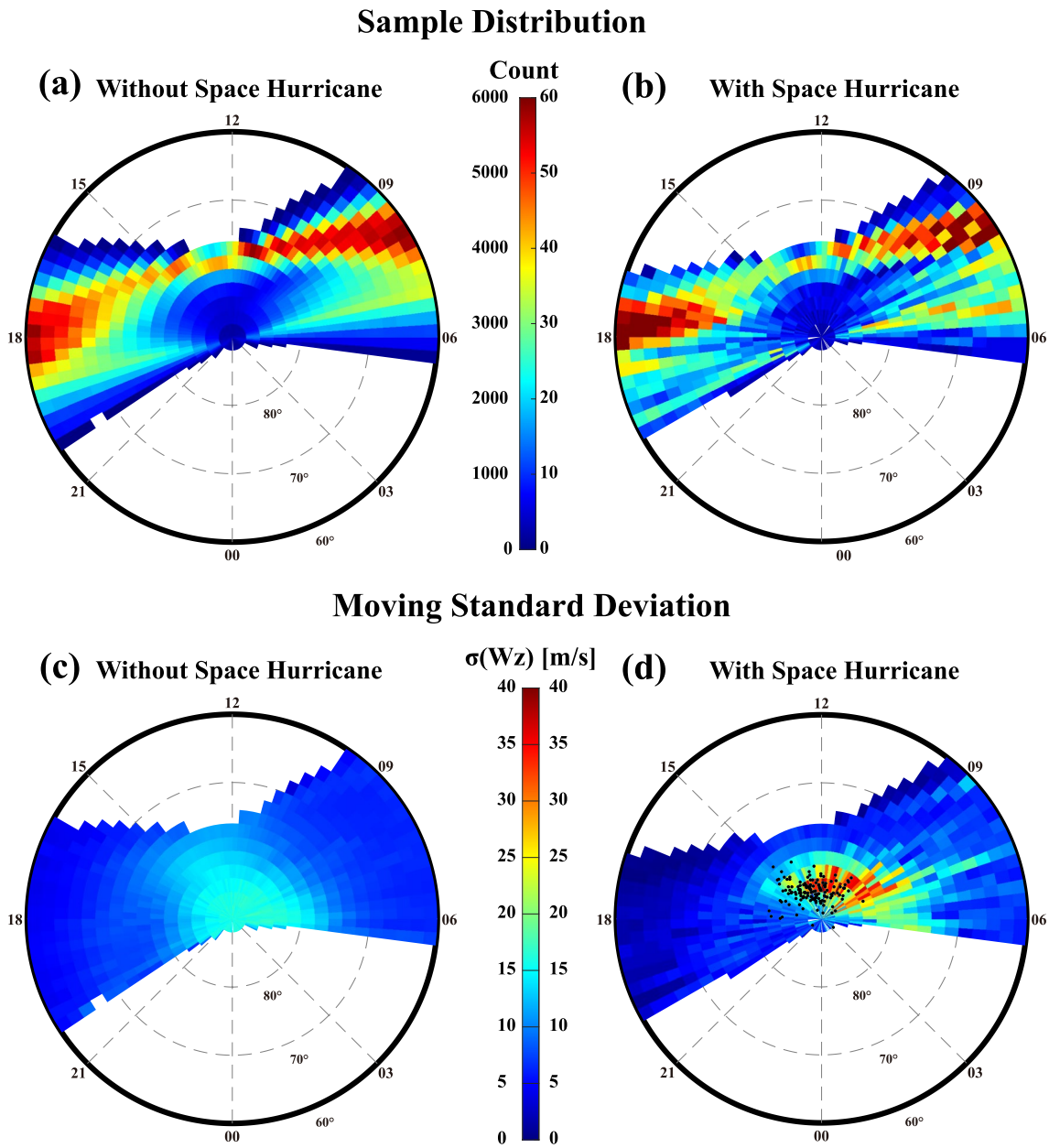

Figure 4. Magnetic Latitude-Magnetic Local Time coordinate (MLT-MLAT) maps of sample distribution (top) and $\sigma(W_z)$ (bottom), binned in 0.25 hr MLT and 2° MLAT. The left column shows the Gravity Field and Steady-State Ocean Circulation Explorer (GOCE) tracks without space hurricane from January 2010 to October 2013. And the right column presents the GOCE tracks with space hurricane. The labels on the left and right side of color bar correspond to without and with space hurricane, respectively. There are 146 space hurricane events observed by Defense Meteorological Satellite Program F16, which center locations indicated by black dots in panel (d).

Data Availability Statement

Data is available at Xiu et al. (2023).

Acknowledgments
This work was supported by the National Natural Science Foundation of China (Grants 42204164, 42120104003 and 42074188), the China Postdoctoral Science Foundation (Grant 2021M701974), the Shandong Provincial Natural Science Foundation (Grants ZR2022QD077, ZR2022MD034), the Chinese Meridian Project, the Stable-Support Scientific Project of China Research Institute of Radiowave Propagation (Grants A132101W02, A132312191), the International Partnership Program of Chinese Academy of Sciences (Grant 183311KYSB20200003), the foundation of National Key Laboratory of Electromagnetic Environment (Grants 6142403180204, 202101001) and Research Council of Norway under contract 223252.

References

Billett, D. D., Hosokawa, K., Grocott, A., Wild, J. A., Aruliah, A. L., Ogawa, Y., et al. (2020). Multi-instrument observations of ion-neutral coupling in the dayside cusp. *Geophysical Research Letters*, *47*(4), e2019GL085590. https://doi.org/10.1029/2019GL085590

Burch, J. L., Reiff, P. H., Spiro, R. W., Heelis, R. A., & Fields, S. A. (1980). Cusp region particle precipitation and ion convection for northward interplanetary magnetic field. *Geophysical Research Letters*. Retrieved from https://agupubs.onlinelibrary.wiley.com/doi/epdf/10.1029/GL007i005p00393

Carter, J. A., Milan, S. E., Fogg, A. R., Sangha, H., Lester, M., Paxton, L. J., et al. (2020). The evolution of long-duration cusp spot emission during lobe reconnection with respect to field-aligned currents. *Journal of Geophysical Research: Space Physics*, *125*(7). https://doi.org/10.1029/2020JA027922

Deng, Y., Fuller-Rowell, T. J., & Ridley, A. J. (2011). Impact of the altitudinal joule heating distribution on the thermosphere. *Journal of Geophysical Research*, *116*(A5). https://doi.org/10.1029/2010ja016019

Deng, Y., Richmond, A. D., Ridley, A. J., & Liu, H. L. (2008). Assessment of the non-hydrostatic effect on the upper atmosphere using a general circulation model (GCM). *Geophysical Research Letters*, *35*(1), 568–569. https://doi.org/10.1029/2007gl032182

Fedorenko, A. K. (2010). Energy balance of acoustic gravity waves above the polar caps according to the data of satellite measurements. *Geomagnetism and Aeronomy*, *50*(1), 107–118. https://doi.org/10.1134/S0016793210010123

Fujii, R., Ozawa, S., Matuura, N., & Brekke, A. (1998). Study on neutral wind contribution to the electrodynamics in the polar ionosphere using EISCAT CP-1 data. *Journal of Geophysical Research*, *103*(A7), 14731–14740.

Guo, J.-P., Deng, Y., Zhang, D.-H., Lu, Y., Sheng, C., & Zhang, S.-R. (2018). The effect of subauroral polarization streams on ionosphere and thermosphere during the 2015 St. Patrick's Day Storm: Global ionosphere-thermosphere model simulations. *Journal of Geophysical Research: Space Physics*, *123*(3), 2241–2256. https://doi.org/10.1002/2017ja024781

Hardy, D. A., Schmitt, L. K., Gussenhoven, M. S., Marshall, F. J., & Yeh, H. C. (1984). Precipitating electron and ion detectors (SSJ/4) for the block 5D/Flights 6–10 DMSP (Defense Meteorological Satellite Program) satellites: Calibration and data presentation. *Rep. AFGL-TR-84-0317. Air Force Geophysics Laboratory*. Retrieved from https://satdat.ngdc.noaa.gov/dmsp/docs/AFGL%20-%201984%20-%20F06-F10%20SSJ4%20Cal%20and%20Data%20-%20AFGL-TR-84-0317.pdf

Hunsucker, R. D. (1982). Atmospheric gravity waves generated in the high-latitude ionosphere: A review. *Reviews of Geophysics*, *20*(2), 293–315. https://doi.org/10.1029/RG020i002p00293

Innis, J. L., & Conde, M. (2001). Thermospheric vertical wind activity maps derived from Dynamics Explorer-2 WATS observations. *Geophysical Research Letters*, *28*(20), 3847–3850. https://doi.org/10.1029/2001gl013704

Innis, J. L., & Conde, M. (2002). Characterization of acoustic-gravity waves in the upper thermosphere using Dynamics Explorer 2 Wind and Temperature Spectrometer (WATS) and Neutral Atmosphere Composition Spectrometer (NACS) data. *Journal of Geophysical Research*, *107*(A12), 1418. https://doi.org/10.1029/2002ja009370

Innis, J. L., Greet, P. A., Murphy, D. J., Conde, M. G., & Dyson, P. L. (1999). A large vertical wind in the thermosphere at the auroral oval/polar cap boundary seen simultaneously from Mawson and Davis, Antarctica. *Journal of Atmosphere and Solar-Terrestrial Physics*, *61*(14), 1047–1058. https://doi.org/10.1016/s1364-6826(99)00060-7

Kiene, A., Bristow, W. A., Conde, M. G., & Hampton, D. L. (2018). Measurements of ion-neutral coupling in the Auroral F region in response to increases in particle precipitation. *Journal of Geophysical Research: Space Physics*, *123*(5), 3900–3918. https://doi.org/10.1002/2017JA024999

Lockwood, M., Milan, S. E., Onsager, T., Perry, C. H., Scudder, J. A., Russell, C. T., & Brittnacher, M. (2001). Cusp ion steps, field-aligned currents and poleward moving auroral forms. *Journal of Geophysical Research*, *106*(A12), 29555–29569. https://doi.org/10.1029/2000JA900175

Lu, S., Xing, Z. Y., Zhang, Q. H., Zhang, Y. L., Ma, Y. Z., Wang, X. Y., et al. (2022). A statistical study of space hurricanes in the Northern Hemisphere. *Frontiers in Astronomy and Space Sciences*, *9*, 1047982. https://doi.org/10.3389/fspas.2022.1047982

Ma, Y. Z., Zhang, Q. H., Xing, Z. Y., Heelis, R. A., Kjellmar, O., & Yong, W. (2018). The ion/electron temperature characteristics of polar cap classical and hot patches and their influence on ion upflow. *Geophysical Research Letters*, *45*(16), 8072–8080. https://doi.org/10.1029/2018gl079099

Milan, S. E., Lester, M., Cowley, S. W. H., & Brittnacher, M. (2000). Dayside convection and auroral morphology during an interval of northward interplanetary magnetic field. *Annales Geophysicae*, *18*(4), 436–444. https://doi.org/10.1007/s00585-000-0436-9

Millward, G. H., Quegan, S., Moffett, R. J., Fuller-Rowell, T. J., & Ree, D. (1993). A modelling study of the coupled ionospheric and thermospheric response to an enhanced high-latitude electric field event. *Planetary and Space Science*, *41*(1), 45–56. https://doi.org/10.1016/0032-0633(93)90016-u

Oyama, S., Ishii, M., Murayama, Y., Shinagawa, H., Buchert, S. C., Fujii, R., & Kofman, W. (2001). Generation of atmosphere gravity waves associated with auroral activity in the polar f-region. *Journal of Geophysical Research*, *106*(A9), 18543–18554. https://doi.org/10.1029/2001ja900032

Oyama, S., & Watkins, B. J. (2012). Generation of atmosphere gravity waves in the polar thermosphere in response to auroral activity. *Space Science Reviews*, *168*(1–4), 463–473. https://doi.org/10.1007/s11214-011-9847-z

Price, G. D., Smith, R. W., & Hernandez, G. (1995). Simultaneous measurements of large vertical winds in the upper and lower thermosphere. *Journal of Atmospheric and Terrestrial Physics*, *57*(6), 631–643. https://doi.org/10.1016/0021-9169(94)00103-u

Rich, F. J., & Hairston, M. (1994). Large-scale convection patterns observed by DMSP. *Journal of Geophysical Research*, *99*(A3), 3827–3844. https://doi.org/10.1029/93JA03296

Shinagawa, H., & Oyama, S. (2006). A two-dimensional simulation of thermospheric vertical winds in the vicinity of an auroral arc. *Earth Planets and Space*, *58*(9), 1173–1181. https://doi.org/10.1186/BF03352007

Sojka, J. J. (2017). Locations where space weather energy impacts the atmosphere. *Space Science Reviews*, *212*(3–4), 1041–1067. https://doi.org/10.1007/s11214-017-0379-z

Stubbe, P., & Chandra, S. (1971). Ionospheric warming by neutral winds. *Planetary and Space Science*, *19*(7), 731–737. https://doi.org/10.1016/0032-0633(71)90031-6

Thayer, J. P., Vickrey, J. F., Heelis, R. A., & Gary, J. B. (1995). Interpretation and modeling of the high-latitude electromagnetic energy flux. *Journal of Geophysical Research*, *100*(A10), 19715–19728. https://doi.org/10.1029/95ja01159

Trinh, Q. T., Ern, M., Doornbos, E., Preusse, P., & Riese, M. (2018). Satellite observations of middle atmosphere-thermosphere vertical coupling by gravity waves. *Annales Geophysicae Atmospheres Hydrospheres & Space Sciences*, *36*(2), 425–444. https://doi.org/10.5194/angeo-36-425-2018

Vennerstrøm, S., Moretto, T., Olsen, N., Friis-Christensen, E., & Watermann, J. F. (2002). Field-aligned currents in the dayside cusp and polar cap region during northward IMF. *Journal of Geophysical Research*, *107*(A8). SMP 18. Retrieved from https://agupubs.onlinelibrary.wiley.com/doi/epdf/10.1029/2001JA009162

Visser, T., March, G., Doornbos, E. N., de Visser, C. C., & Visser, P. N. A. M. (2019). Characterization of thermospheric vertical wind activity at 225-km to 295-km altitude using GOCE data and validation against Explorer missions. *Journal of Geophysical Research: Space Physics*, *124*(6), 4852–4869. https://doi.org/10.1029/2019ja026568

Xiu, Z. F., Ma, Y. Z., Zhang, Q. H., Xing, Z. Y., Zhang, S. R., Zhang, Y. L., et al. (2023). Geomagnetic data, DMSP\SSUSI data and GOCE thermosphere data on 15th June 2010 and the statistical results of GOCE from January 2010 to October 2013 [Dataset]. Zenoto. https://doi.org/10.5281/zenodo.10001510

Zhang, Q. H., Zhang, Y. L., Wang, C., Oksavik, K., Lyons, L. R., Lockwood, M., et al. (2021). A space hurricane over the Earth's polar ionosphere. *Nature Communications*, *12*(1), 1207. https://doi.org/10.1038/s41467-021-21459-y

Zhang, S.-R., Erickson, P. J., Coster, A. J., Rideout, W., Vierinen, J., Jonah, O., & Goncharenko, L. P. (2019). Subauroral and polar traveling ionospheric disturbances during the 7–9 September 2017 storms. *Space Weather*, *17*(12), 1748–1764. https://doi.org/10.1029/2019SW002325

Zhang, S.-R., Erickson, P. J., Goncharenko, L. P., Coster, A. J., Rideout, W., & Vierinen, J. (2017). Ionospheric bow waves and perturbations induced by the 21 August 2017 solar eclipse. *Geophyical Research Letters*, *44*(24), 12–067. https://doi.org/10.1002/2017GL076054